Electronic Density of States and Transport Properties for 2D Heterostructures

Mitchell Luskin
Daniel Massatt and Christoph Ortner
Paul Cazeaux and Eric Cancès
Stephen Carr, Shiang Fang, and Efthimios Kaxiras
Hyobin Yoo and Philip Kim

University of Minnesota -Twin Cities
University of Warwick
Ecole des Pont
Harvard University

May 3, 2017

Cornocupia of 2D materials

Graphene

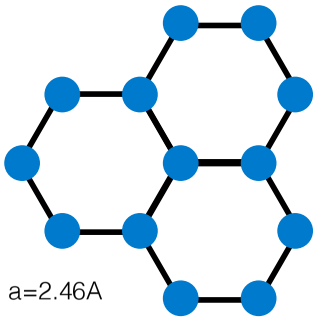

Semimetal

- Dirac cone: linear dispersion
- Inversion symmetry
- Extraordinary properties (mechanical strength, etc.)

Hexagonal Boron Nitride (hBN)

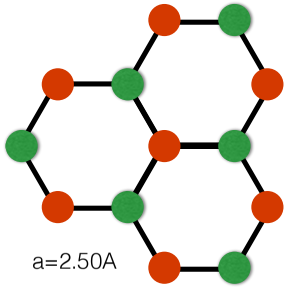

Insulator

- Broken inversion symmetry
- Large band gap, 5eV
- Stability
- Used to encapsulate graphene

Semiconductors

Transition Metal Dichalcogenides

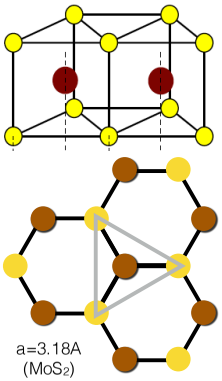

- MX_2, M: Mo/W, X = S/Se/Te
- Broken inversion symmetry
- Direct band gap, 1-2eV at K valleys
- Spin-orbit coupling

Phosphorene / Black phosphorus

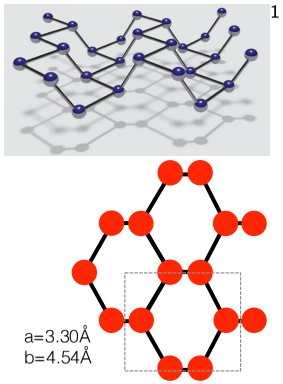

- Anisotropy (rectangular lattice)
- Direct band gap, 2eV (.3eV bulk)
- Relatively reactive

Motivation

- Stacking assemblies of 2D materials:

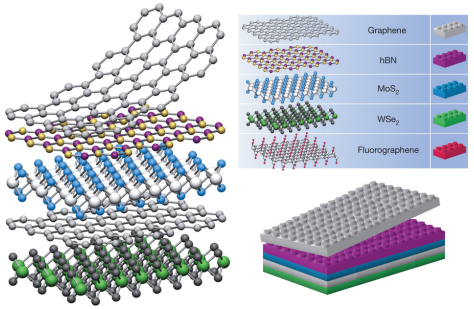

[*Van der Waals heterostructures*, Geim & Grigorieva, *Nature* '13]

- Building blocks to custom properties.
- **Incommensurate lattices**, twists, defects, domain boundaries.
- How to predict **electronic, optical properties**?

Motivation

- Stacking assemblies of 2D materials:

- Building blocks to custom properties.
- **Incommensurate lattices**, twists, defects, domain boundaries.
- How to predict **electronic, optical properties**?

Stacked 2D Heterostuctures: No Periodic Structure

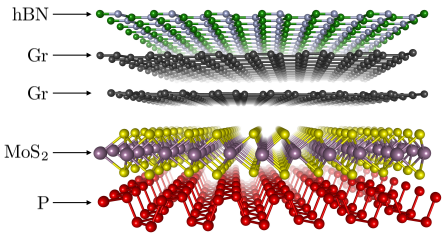

Example of heterostructure with five monolayers

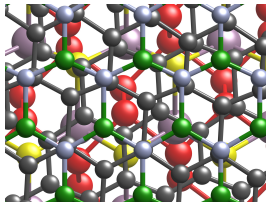

Top view of the atomic structure

Unrotated and Rotated Bilayer MoS_2.

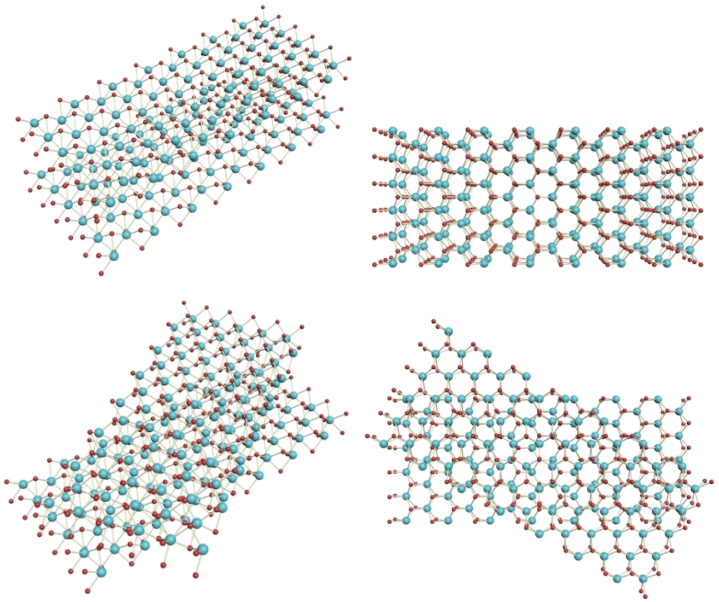

Rotated Bilayer Graphene

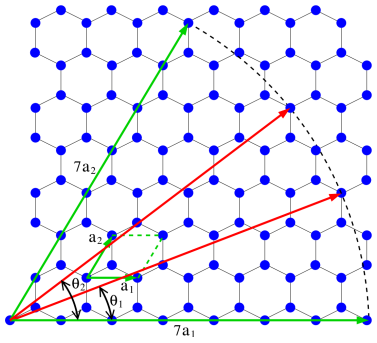

Structure of single-layer graphene with blue circles representing atomic positions.

Rotated vectors of equal magnitude with non-trivial orientation in red arrows give commensurate (existence of periodic supercell) rotations.

The two possible rotation angles, θ_1, θ_2 are indicated.

Commensurate angles are dense, but supercell (fundamental domain) becomes arbitrarily large for small angles.

Upscaling: a hierarchy of models

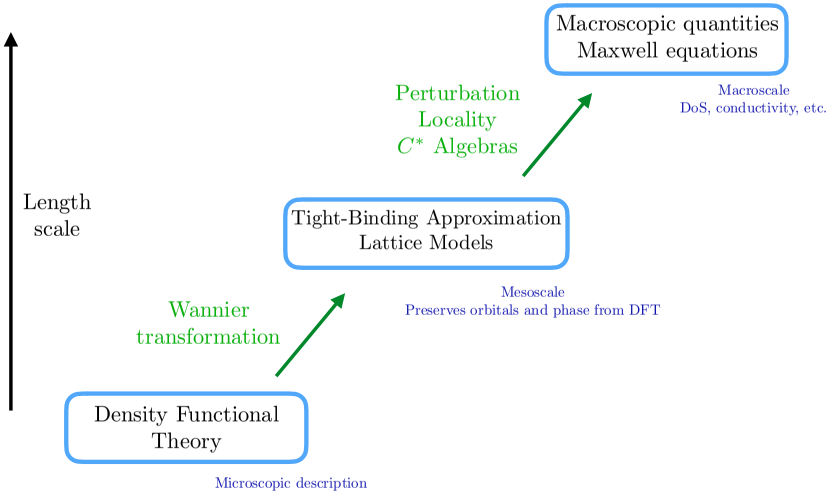

Computational Goals

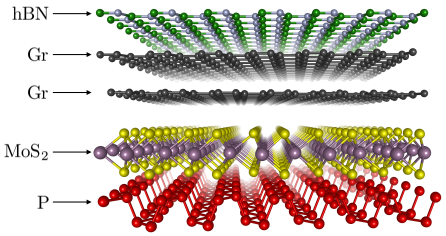

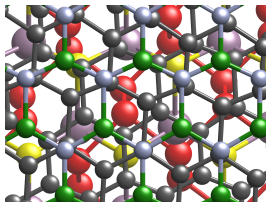

Top view of the atomic structure

- Current methods approximate incommensurate structures by supercells:
  - Size increases quickly for low angle twist, very expensive calculations
  - Uncontrolled and unknown error
- New methods sample configurations, exploit locality
  - Can efficiently compute full parameter space, even low angle twist
  - Efficient theory-based numerical methods with controlled and known error

2D bilayer geometry

For sheet $j \in \{1,2\}$, we define the Bravais lattice

$$\mathcal{R}_j = \{A_j n : n \in \mathbb{Z}^2\}$$

where A_j is a 2×2 invertible matrix. We define the *unit cell* for sheet j as

$$\Gamma_j = \{A_j x : x \in [0,1)^2\}.$$

Each individual sheet is trivially periodic, since

$$\mathcal{R}_j = A_j n + \mathcal{R}_j \qquad \text{for } n \in \mathbb{Z}^2.$$

The combined system $\mathcal{R}_1 \cup \mathcal{R}_2$ need not be periodic, though.

Represent multilattices by $\mathcal{R}_1 \times \mathcal{A}_1$ and $\mathcal{R}_2 \times \mathcal{A}_2$.

Local Geometry of rotated bilayer graphene

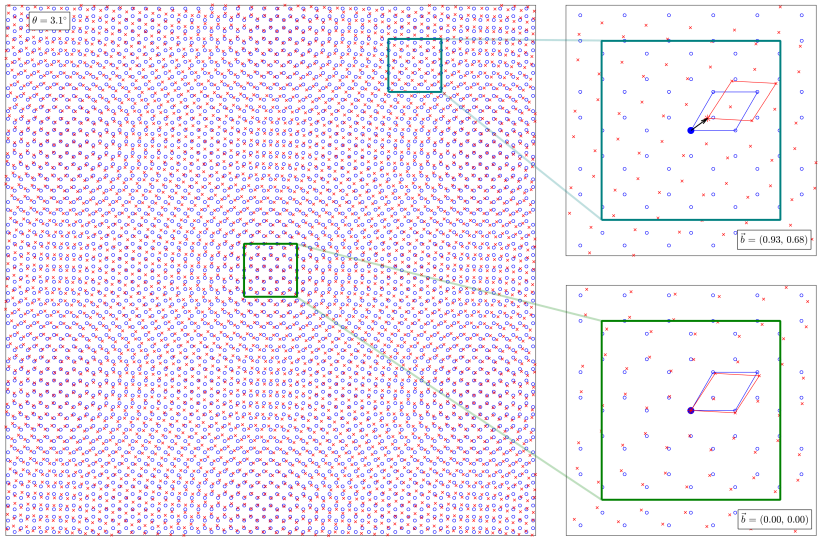

Blue-orbital's local environment described completely by the "$\vec{b}$-shift" between the blue and red unit-cells.

Equidistribution of lattice shifts (Ergodicity)

Let $\mathcal{R}_1$ and $\mathcal{R}_2$ be incommensurate lattices embedded in $\mathbb{R}^2$:

$$v + \mathcal{R}_1^* \cup \mathcal{R}_2^* = \mathcal{R}_1^* \cup \mathcal{R}_2^* \quad \Leftrightarrow \quad v = \begin{pmatrix} 0 \\ 0 \end{pmatrix}.$$

Equivalent to absence of constructive Bragg reflections.

Let P_j be the transposition of 1 and 2, that is, $P_1 = 2$ and $P_2 = 1$.

Theorem

For $h \in C_{per}(\Gamma_{P_j})$, we have

$$\frac{1}{\#\mathcal{R}_j \cap B_r} \sum_{\ell \in \mathcal{R}_j \cap B_r} h(\ell) \to \frac{1}{|\Gamma_{P_j}|} \int_{\Gamma_{P_j}} h(b) db.$$

Local geometries around sheet 1 sites can be parameterized by Γ_2.

Local geometries around sheet 2 sites can be parameterized by Γ_1.

Tight-Binding Model

Tight-binding parameterizes the Hamiltonian into interactions between localized basis functions:

$$h_{\alpha\alpha'}(R - R') \sim \langle \phi_{(R,\alpha)} | \mathcal{H} | \phi_{(R',\alpha')} \rangle.$$

We can formally define an operator H such that

$$H_{R\alpha,R'\alpha'} = h_{\alpha\alpha'}(R - R'),$$

and an eigenproblem

$$H\psi = E\psi.$$

The operator H does not have translation symmetry and thus cannot diagonalized by a Bloch transform if $\mathcal{R}_1 \cup \mathcal{R}_2$ is not periodic.

- We assume an exponential localization of the Hamiltonian entries:

$$|h_{\alpha\alpha'}(x)| \leqslant Ce^{-\tilde{\gamma}|x|}.$$

From DFT to Tight-Binding Models: Wannier transformation

- Spectral projection,
- Localized basis:

Wannier orbitals.

- Reproduce band structure (within an energy window)
- Effective reduced model

N. Marzari & D. Vanderbilt '97

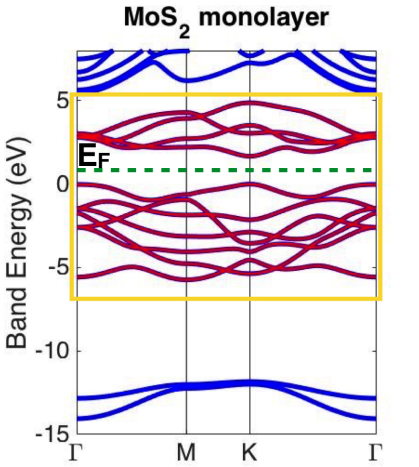

DFT / TBH

Ab-initio tight-binding Hamiltonian for transition metal dichalcogenides
S. Fang, R. Kuate Defo, S. Shirodkar, S. Lieu, G. Tritsaris, and E. Kaxiras, PRB '15

Interlayer coupling terms

Angular decomposition for Coupling

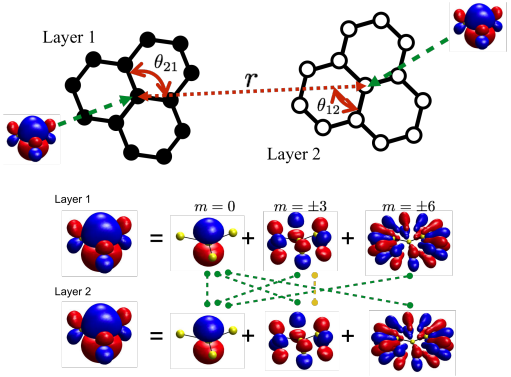

$$t(r) = V_0(r) + V_3(r)(cos(3\theta_{12}) + cos3\theta_{21}) + V_6(r)(cos(6\theta_{12}) + cos6\theta_{21}).$$

Main ideas:

- Need for systematic library,
- Transferable (twist angle...)

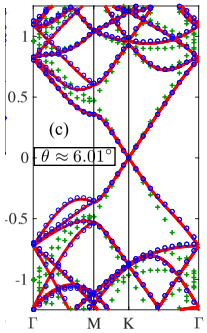

Graphene bilayer band structure, 6x5 supercell

Electronic Structure Theory of Weakly Interacting Bilayers, S. Fang & E. Kaxiras, PRB '16

Density of States Approximation

For $\tilde{\Omega} \subset \Omega := \mathcal{R}_1 \times \mathcal{A}_1 \cup \mathcal{R}_2 \times \mathcal{A}_2$. with $\#\tilde{\Omega} = n$, the associated Hamiltonian is

$$\tilde{H} = (H_{ij})_{i,j \in \tilde{\Omega}} \in \mathbb{C}^{n \times n}.$$

The density of states for $\tilde{\Omega}$ can be defined via its action on test functions, or, observables g, by

$$\mathcal{D}[\tilde{H}](g) = \frac{1}{n} \mathrm{Tr}[g(\tilde{H})], \qquad g \in C(\mathbb{R}).$$

The local density of states distribution is defined as

$$\mathcal{D}_k[\tilde{H}](g) = [g(\tilde{H})]_{kk}, \qquad k \in \tilde{\Omega},\ g \in C(\mathbb{R}).$$

Note that

$$\frac{1}{n} \sum_{k \in \tilde{\Omega}} \mathcal{D}_k[\tilde{H}](g) = \mathcal{D}[\tilde{H}](g).$$

Local DoS Approximation

We now specify finite domains

$$\tilde{\Omega} = \Omega_r := \big[\mathcal{R}_1 \cap B_r\big]\times\mathcal{A}_1 \;\cup\; \big[\mathcal{R}_2 \cap B_r\big]\times\mathcal{A}_2, \qquad \text{for } r > 0.$$

For $r > 0$ and $b \in \mathbb{R}^2$ we define $H_{r,j}(b) \in \mathbb{C}^{|\Omega_r|\times|\Omega_r|}$ by

$$[H_{r,j}(b)]_{R\alpha,R'\alpha'} = h_{\alpha\alpha'}\big(b(\delta_{\alpha\in\mathcal{A}_{P_j}} - \delta_{\alpha'\in\mathcal{A}_{P_j}}) + R - R'\big), \quad R\alpha, R'\alpha' \in \Omega_r.$$

$H_{r,j}(b)$ describes a cluster of radius r in which the sheet P_j is shifted by b. Then

$$\mathcal{D}_\alpha[H_{r,j}(b)] := \mathcal{D}_{0\alpha}[H_{r,j}(b)] \quad \text{for} \quad \alpha \in \mathcal{A}_j$$

is an approximate local density of states distribution of the infinite system at a local configuration indexed by $b \in \Gamma_{P_j}$ at orbital α on sheet j.

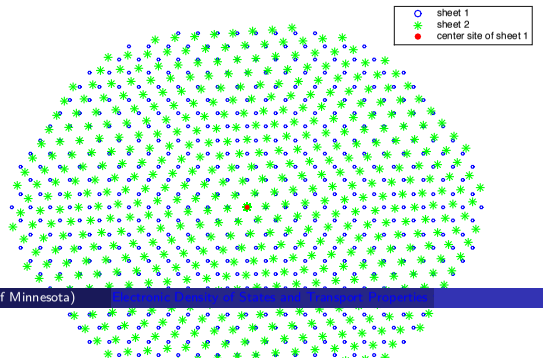

Spectrum and Observables

Let

$$E[H] := \sup_{r>0,\, j\in\{1,2\}} \left[\sup_{b\in\Gamma_j} \|H_{r,j}(b)\|_2 \right] < \infty,$$

where

$$\|\tilde{H}\|_2 := \sup_{\psi\in\mathbb{C}^n\setminus\{0\}} \|\tilde{H}\psi\|_2/\|\psi\|_2 \quad \text{for} \quad \tilde{H}\in\mathbb{C}^{n\times n}.$$

Then the local density of states distribution will be supported on the space

$$S[H] = [-E[H], E[H]].$$

We define the admissible test functions

$$\Lambda := \{g \in C(\mathbb{R}) \mid \ g \text{ is analytic on } S[H]\}.$$

If $g \in \Lambda$, then there exists $\tilde{d} > 0$ such that $g \in \Lambda_{\tilde{d}}$, which is defined as

$$\Lambda_{\tilde{d}} := \{g \in C(\mathbb{R}) \mid \ g \text{ is analytic at } z \text{ for } d(z, S[H]) \leqslant \tilde{d}\}.$$

Thermodynamic Limit

Theorem

(1) For $\alpha \in \mathcal{A}_j$, there exists a function $\mathcal{D}_\alpha[H] : \Gamma_{P_j} \times C(S[H]) \to \mathbb{C}$ such that, for any $g \in \Lambda$,

$$\mathcal{D}_\alpha[H_{r,j}(b)](g) \to \mathcal{D}_\alpha[H](b,g) \quad \text{as } r \to \infty.$$

The distribution $\mathcal{D}_\alpha[H](b,g)$ is the local density of states for the infinite system.

(2) The map $g \mapsto \mathcal{D}_\alpha[H](b,g)$ is a bounded linear functional, more precisely,

$$\left|\mathcal{D}_\alpha[H](b,g)\right| \leqslant \|g\|_\infty.$$

(3) There exist constants $C, \gamma' > 0$ such that, for $\tilde{d} > 0$ and $g \in \Lambda_{\tilde{d}}$,

$$|\mathcal{D}_\alpha[H](b,g) - \mathcal{D}_\alpha[H_{r,j}(b)](g)| \leqslant C\tilde{d}^{-6} \sup_{d(z,S[H])<\tilde{d}} |g(z)| e^{-\gamma' \tilde{d} r}.$$

Thermodynamic Limit

We next analyze the regularity of the map $b \mapsto \mathcal{D}_\alpha[H](b, g)$ for fixed g, which will allow us to integrate with respect to b.

Theorem

Suppose $h_{\alpha\alpha'} \in C_0^n(\mathbb{R}^2)$ *for* $n \in \mathbb{N} \cup \{\infty\}$. *Then, for* $\alpha \in \mathcal{A}_j$ *and* $g \in \Lambda$,

$$\mathcal{D}_\alpha[H](\cdot, g) \in C^n_{\mathrm{per}}(\Gamma_{P_j}).$$

Thermodynamic Limit

Theorem

There exists a bounded linear functional $\mathcal{D}[H] : C(S[H]) \to \mathbb{C}$ *such that for* $g \in \Lambda$, *we have*

$$\mathcal{D}[H_{r,j}(0)](g) \to \mathcal{D}[H](g) \quad \text{as } r \to \infty, \quad \text{for } j = 1, 2,$$

and

$$\mathcal{D}[H](g) = \nu \sum_{j=1}^{2} \sum_{\alpha \in \mathcal{A}_j} \int_{\Gamma_{P_j}} \mathcal{D}_\alpha[H](b, g) db,$$

where

$$\nu = \frac{1}{|\mathcal{A}_2| \cdot |\Gamma_1| + |\mathcal{A}_1| \cdot |\Gamma_2|}.$$

If $g \in \Lambda_{\tilde{d}}$, *we have the explicit error bound*

$$\left| \mathcal{D}[H](g) - \nu \sum_{j=1}^{2} \sum_{\alpha \in \mathcal{A}_j} \int_{\Gamma_{P_j}} \mathcal{D}_\alpha[H_{r,j}(b)](g) db \right| \leqslant C \tilde{d}^{-6} \sup_{d(z, S[H]) < \tilde{d}} |g(z)| e^{-\gamma \tilde{d} r}.$$

Quadrature

Theorem

Assume $h_{\alpha\alpha'}$ is analytic. Let

$$S_j = \left\{ A_j \begin{pmatrix} i_1/N_{disc} \\ i_2/N_{disc} \end{pmatrix} : 0 \leqslant i_1, i_2 < N_{disc} \right\}$$

be the uniform discretization sample points for Γ_j. Then we have

$$\left| \frac{|\Gamma_{P_j}|}{N_{disc}^2} \sum_{b \in S_{P_j}} \sum_{\alpha \in \mathcal{A}_j} \mathcal{D}_\alpha[H](b,g) - \sum_{\alpha \in \mathcal{A}_j} \int_{\Gamma_{P_j}} \mathcal{D}_\alpha[H](b,g) db \right| \leqslant C \tilde{d}^{-1} \sup_{z:\ d(z,S[H]) < \tilde{d}} |g(z)| e^{-\gamma'' \tilde{d} N_{disc}}$$

for some $\gamma'' > 0$.

Proofs

We can write for $\tilde{\Omega} \subset \Omega$ finite, $\tilde{H} \in \mathbb{C}^{|\tilde{\Omega}| \times |\tilde{\Omega}|}$, $k \in \tilde{\Omega}$, and g analytic

$$[g(\tilde{H})]_{kk} = \frac{1}{2\pi i} \oint_{\mathbb{C}} g(z)[(z - \tilde{H})^{-1}]_{kk} dz,$$

where $\mathbb{C}$ is a contour around $S[H]$ which contains the spectrum.

We then rely on Coombe–Thomas decay estimates for $[(z - \tilde{H})^{-1}]_{kk}$ as $\tilde{\Omega} \uparrow \Omega$.

Kernel Polynomial Method Approximation

An eigensolve on $H_{r,j}(b)$ for each quadrature point b is computationally expensive, with scaling $O(r^6)$ for a single shift in b.

We use the Kernel Polynomial Method (KPM) with Chebyshev polynomials to compute the density of states with scaling $O(r^2)$ for each single shift in b.

It yields the density of states operator as a smooth function from which multiple observables can then be computed.

Kernel Polynomial Method Approximation

An approximation to the shifted delta function $\delta(e-\varepsilon)$, at $\varepsilon \in (-1,1)$, is given by

$$\hat{\chi}_p(\varepsilon, e) = \frac{1}{\pi\sqrt{1-\varepsilon^2}} \sum_{m \leqslant p} g_m^p T_m(\varepsilon) T_m(e), \qquad e, \varepsilon \in (-1,1),$$

where

$$g_m^p = (2-\delta_{m0}) \frac{(p-m+1)\cos(\frac{\pi m}{p+1}) + \sin(\frac{\pi m}{p+1})\arctan(\frac{\pi}{p+1})}{p+1}$$

are the so-called Jackson coefficients designed to remove the Gibbs phenomenon.

To approximate the density of states on the interval $S[H] = [-E[H], E[H]]$, we rescale

$$\chi_p(\varepsilon, e) := \eta \hat{\chi}_p(\eta\varepsilon, \eta e), \qquad e, \varepsilon \in (-1/\eta, 1/\eta),$$

where η is a positive constant selected so that $E[H] \leqslant 1/\eta$.

Kernel Polynomial Method Approximation

We will approximate $\mathcal{D}[H]$ by

$$\mathcal{D}_{\chi_p}(\varepsilon) = \nu \sum_{j=1}^{2} \sum_{\alpha \in \mathcal{A}_j} \int_{\Gamma_{P_j}} \mathcal{D}_\alpha[H](b, \chi_p(\varepsilon, \cdot)) db,$$

and subsequently approximate the integrand $\mathcal{D}_\alpha[H](b, \chi_p(\varepsilon, \cdot))$ by

$$\begin{aligned} \mathcal{D}_\alpha[H_{r,j}(b)](\chi_p(\varepsilon, \cdot)) &= [\chi_p(\varepsilon, H_{r,j}(b))]_{0\alpha,0\alpha} \\ &\approx \frac{\eta}{\pi\sqrt{1-(\eta\varepsilon)^2}} \sum_{m \leqslant p} g_m^p T_m(\eta\varepsilon) \left[\eta T_m(H_{r,j}(b))\right]_{0\alpha,0\alpha}. \end{aligned}$$

Note that for all ε, the calculation requires the same $[T_m(\eta H_{r,j}(b))]_{0\alpha,0\alpha}$ coefficients, which can be calculated efficiently by matrix-vector products using the Chebyshev recursion.

Kernel Polynomial Method Approximation

Theorem

We have for $g \in \Lambda_{\tilde{d}}$ that

$$\left|\mathcal{D}[H](g) - \int \mathcal{D}(\varepsilon) g(\varepsilon) d\varepsilon\right| \leqslant \underbrace{C\tilde{d}^{-6} \sup_{d(z,S[H])<\tilde{d}} |g(z)| e^{-\gamma \tilde{d} r}}_{\text{Truncation Error}} + \underbrace{C\tilde{d}^{-1} \sup_{d(z,S[H])<\tilde{d}} |g(z)| e^{-\gamma' \tilde{d} N_{disc}}}_{\text{Discretization Error}} + \underbrace{C' \left\| g - \int \chi_p(\varepsilon, \cdot) g(\varepsilon) d\varepsilon \right\|_\infty}_{\text{Kernel Polynomial Method Error}}.$$

The errors will be balanced if

$$r \sim N_{\text{disc}} \sim p \log(p).$$

Numerical Results

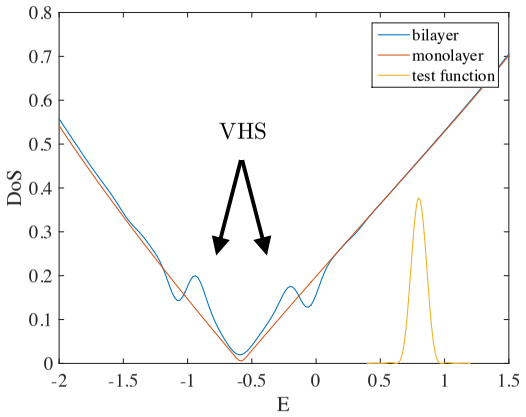

Figure: Approximation of the DoS using with $r = 180$, $p = 700$, and $N_{\text{disc}} = 4$. We can see Van Hove Singularities (VHS) forming near the Dirac Point, agreeing with theoretical results. We include the test function $(\chi_p(\varepsilon, \cdot))$, which is to scale in the E-axis, but not in the DoS-axis.

Twisted Bilayer Graphene Calculation

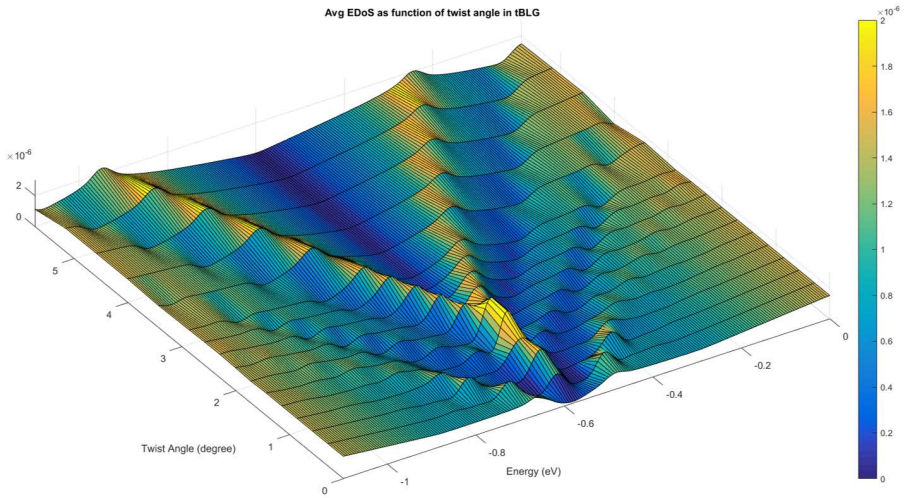

Figure: 500 Angstrom radius disk (600,000 atoms in total)

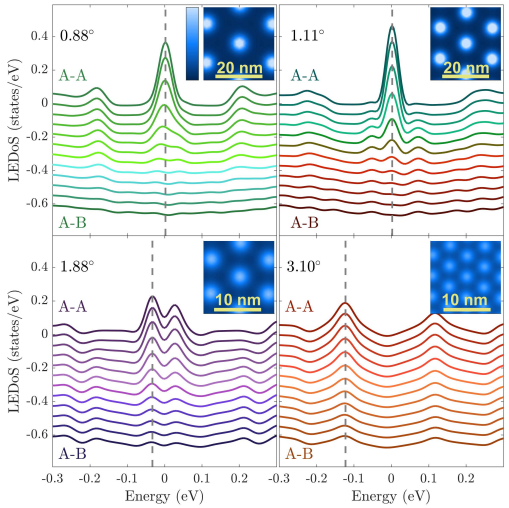

Figure: Simulated local electronic density of states (LEDoS) of four different angles of twisted bilayer graphene. Each line corresponds to a different real-space configuration along the line connecting A-A to A-B stacking. The insets show a real-space image of the density of states in the bilayer system at the energy value identified by a dashed line.

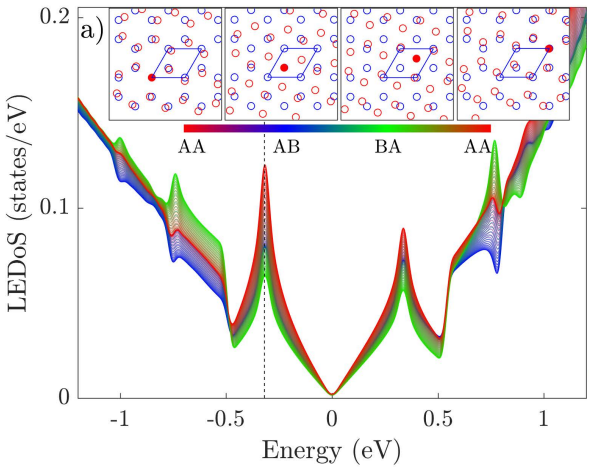

Figure: Local Electronic Density of States as a function of shift distance across the unit cell diagonal: (a) Scan of a single orbital's LEDoS with the coloring corresponding to distance across the diagonal. The insets show the real-space configurations ω for three types of stacking with the bottom layer atoms represented by blue circles and the top layer ones by red circles. The unit-cell of the bottom layer is outlined in blue and the shifted orbital is highlighted as a filled red dot.

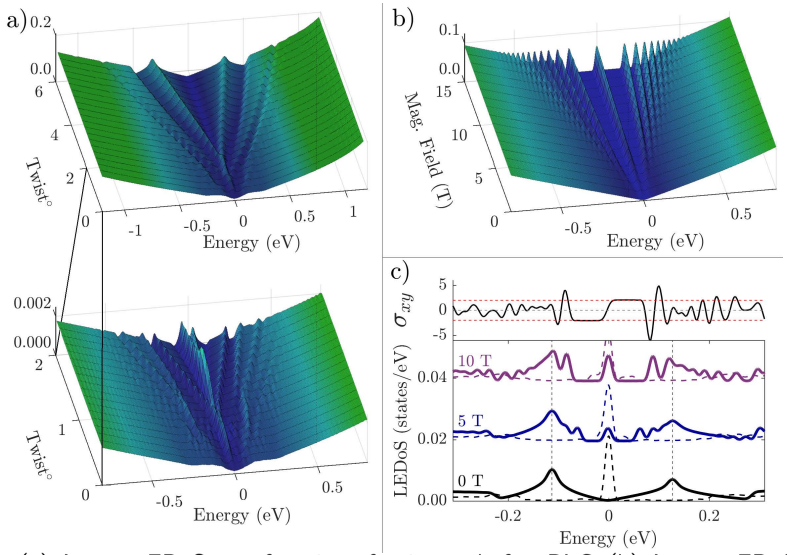

Figure: (a) Average EDoS as a function of twist angle for tBLG. (b) Average EDoS for monolayer graphene in the presence of varying magnetic field. (c) LEDoS for AA stacked tBLG with 3.1° (solid line) and 1.1° (dashed line) twist-angle and different values of magnetic field and Hall conductivity σ_{xy} in units of e^2/h, with the horizontal red dashed lines at $\pm 2e^2/h$ for 3.1° twist .

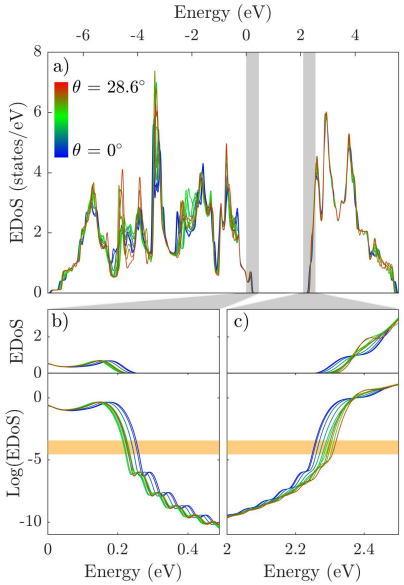

Figure: EDoS for twisted bilayer MoS_2 from 0° (blue) to 28.65° (red) twist angle. The gap widens by 76 meV when going from a 0° to 28.65° twist angle (a 4% relative increase in the band gap).

Tight-binding C^*-algebra

Tight-binding models in a nutshell

- Discrete description: fixed lattice $\mathcal{R}$,
- Single-electron picture,
- **Quantum states**: wave function

$$\psi \in \ell^2(\mathcal{R}, \mathbb{C})$$

- $|\psi(\mathbf{n})|^2$: probability of electron at $\mathbf{n}$,
- **Linear operators**: observables

$$H\psi(\mathbf{n}) = \sum_{\mathbf{m}\in\mathcal{R}} H(\mathbf{n},\mathbf{m})\psi(\mathbf{m}).$$

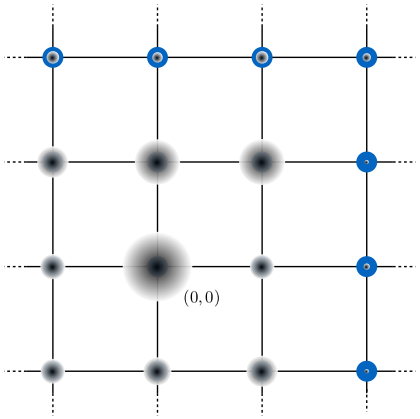

- Periodic operators are easy to parameterize:

$$H(\mathbf{n},\mathbf{m}) = h(\mathbf{m}-\mathbf{n}), \qquad \text{with } h:\ \mathcal{R} \mapsto \mathbb{C}.$$

Tight-binding models in a nutshell

- Discrete description: fixed lattice $\mathcal{R}$,
- Single-electron picture,
- **Quantum states**: wave function

$$\psi \in \ell^2(\mathcal{R}, \mathbb{C})$$

- $|\psi(\mathbf{n})|^2$: probability of electron at $\mathbf{n}$,
- **Linear operators**: observables

$$H\psi(\mathbf{n}) = \sum_{\mathbf{m}\in\mathcal{R}} H(\mathbf{n},\mathbf{m})\psi(\mathbf{m}).$$

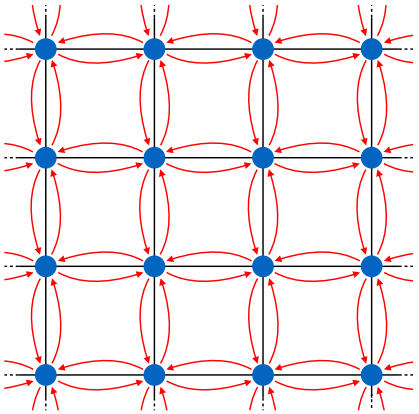

- Periodic operators are easy to parameterize:

$$H(\mathbf{n},\mathbf{m}) = h(\mathbf{m}-\mathbf{n}), \qquad \text{with } h:\ \mathcal{R} \mapsto \mathbb{C}.$$

Tight-binding models in a nutshell

- Discrete description: fixed lattice $\mathcal{R}$,
- Single-electron picture,
- **Quantum states**: wave function

$$\psi \in \ell^2(\mathcal{R}, \mathbb{C})$$

- $|\psi(\mathbf{n})|^2$: probability of electron at $\mathbf{n}$,
- **Linear operators**: observables

$$H\psi(\mathbf{n}) = \sum_{\mathbf{m}\in\mathcal{R}} H(\mathbf{n},\mathbf{m})\psi(\mathbf{m}).$$

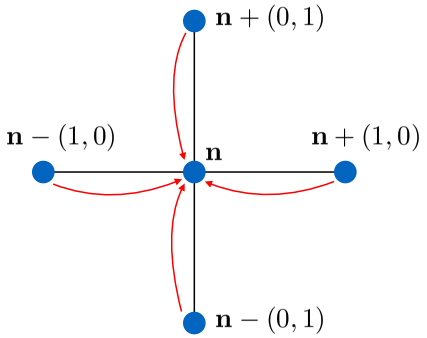

- Periodic operators are easy to parameterize:

$$H(\mathbf{n},\mathbf{m}) = h(\mathbf{m}-\mathbf{n}), \qquad \text{with } h:\ \mathcal{R}\mapsto\mathbb{C}.$$

The special case of a periodic crystal

Assume a periodic lattice $\mathcal{R}$ and a single orbitals per site.

Smallest set of interesting periodic observables:

$$\mathcal{A}_0 = \{f : \mathcal{R} \to \mathbb{C} \mid f \text{ has compact support on } \mathcal{R}\}$$

- Representation as periodic operators on $\ell^2(\mathcal{R})$:

$$[\pi(f)](\mathbf{n}, \mathbf{m}) = f(\mathbf{m} - \mathbf{n}).$$

- Addition, multiplication:

$$(f + g)(\mathbf{n}) = f(\mathbf{n}) + g(\mathbf{n}), \qquad (f * g)(\mathbf{n}) = \sum_{\mathbf{m} \in \mathcal{R}} f(\mathbf{m}) g(\mathbf{n} - \mathbf{m}),$$

- Norm, $*$-operation:

$$\|f\| = \|\pi(f)\|, \qquad f^*(\mathbf{n}) = \overline{f(-\mathbf{n})}.$$

The C^*-algebra of observables $\mathcal{A}$ is then the completion of $\mathcal{A}_0$ for the norm $\|\cdot\|$.

Observables and C^*-algebras of operators

Algebra $\mathcal{A}$ (addition, multiplication, scalar multiplication), further equipped with

- A norm such that $\mathcal{A}$ is complete in the norm topology and

$$\|f * g\| \leqslant \|f\| \cdot \|g\|, \qquad \forall f, g \in \mathcal{A},$$

- An antilinear $*$-operation such that

$$(f * g)^* = g^* * f^*, \quad \|f * f^*\| = \|f\|^2, \qquad \forall f, g \in \mathcal{A}.$$

- A C^* algebra encodes **operators** (observables)!

Non-commutative geometry extends crucial tools to aperiodic media such as:

- Integration over the Brillouin zone,
- Derivation w.r.t the quasimomentum $\mathbf{k}$,
- Spectral analysis,
- Functional calculus...

Identify Ω: the space of configurations instead of the Brillouin zone Γ^*.

[J. Bellissard, A. van Elst, H. Schulz-Baldes, Math. Phys '94]

[E. Prodan, Appl. Math. Express '12]

Incommensurate systems and noncommutative algebras. Modeling electronic transport

Relevant publications:

- [E. Cancès, P. Cazeaux, M. Luskin. *Generalized Kubo Formulas for the Transport Properties of Incommensurate 2D Atomic Heterostructures.* Submitted]
- [S. Carr, D. Massatt, P. Cazeaux, S. Fang, M. Luskin, and E. Kaxiras. *Twistronics: Manipulating the electronic properties of two-dimensional layered structures through their twist angle.* Submitted]

Incommensurate multilayer systems

- Vertical stack of p d-dimensional layers in $\mathbb{R}^{d+1}$, $d = 1, 2$.
- No periodic structure, but long-range order.
- Notion of homogeneity.

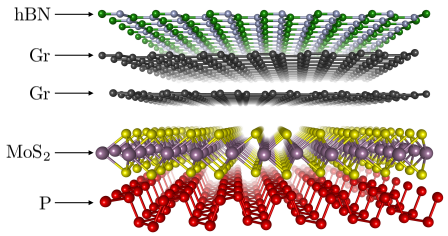

Example of heterostructure with five monolayers

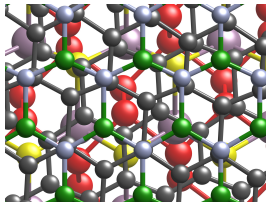

Top view of the atomic structure

A few notations:

- $\mathcal{R}_j$ the d-dimensional lattice of layer j,
- $\Gamma_j := \mathbb{R}^d/\mathcal{R}_j$ the d-dimensional periodic unit cell of layer j.

Geometry of multilayer systems

Abstract construction: [The Noncommutative Geometry of Aperiodic Solids, J. Bellissard '01].

- Nuclear charge density: Radon measure ρ_{nuc} in $\mathfrak{M}(\mathbb{R}^{d+1})$,
- Natural action of $\mathbb{R}^d$ as in-plane translations $T_{\mathbf{a}}$,
- Ω: orbit closure of ρ_{nuc} under the $\mathbb{R}^d$-action,
- Dynamical system $(\Omega, \mathbb{R}^d, T)$: **the hull**.

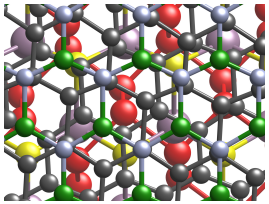

Top view of the atomic structure

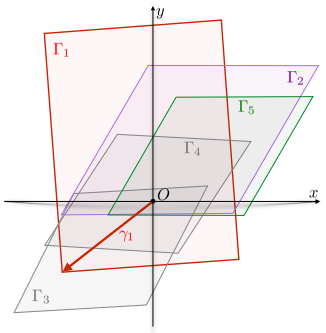

Origin projected into the unit cells

Natural parameterization:

$$\Omega \subset \Gamma_1 \times \cdots \times \Gamma_p.$$

Defining incommensurability

- Periodic case: Ω d-dimensional torus (Supercell)
  $\rightsquigarrow$ embedded in $\Gamma_1 \times \cdots \times \Gamma_p$ (dimension $p \times d$)
- Incommensurate case $\rightsquigarrow$ Ergodicity!

Lattices $\mathcal{R}_1, \cdots, \mathcal{R}_p$ are **incommensurate** if

$$\forall (\mathbf{K}_1, \ldots, \mathbf{K}_p) \in \mathcal{R}_1^* \times \cdots \times \mathcal{R}_p^*, \qquad \sum_{j=1}^{p} \mathbf{K}_j = \mathbf{0} \quad \Leftrightarrow \quad \mathbf{K}_j = \mathbf{0} \quad \forall j = 1, \ldots, p.$$

- Equivalent to absence of constructive Bragg reflections.

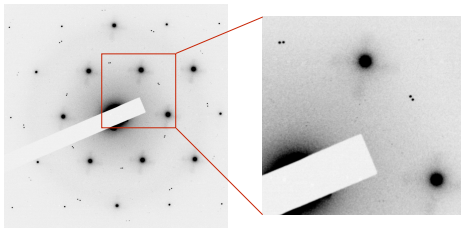

Ergodicity: averaging functions

- We define the hull $\Omega = \Gamma_1 \times \cdots \times \Gamma_p$.
- Action of $\mathbb{R}^d$ on Ω:

$$\omega = (\gamma_1, \ldots, \gamma_p): \qquad T_{\mathbf{a}}\omega = (\gamma_1 + \mathbf{a}, \ldots, \gamma_p + \mathbf{a}).$$

Proposition (P. Cazeaux, E. Cancès, M. Luskin)

$\mathbb{P}$: uniform probability distribution on Ω.

- $\mathbb{P}$ is invariant by the translation group $\mathbb{R}^d$.
- The dynamical system $(\Omega, \mathbb{R}^d, T, \mathbb{P})$ is ergodic iff $\mathcal{R}_1, \cdots, \mathcal{R}_p$ are incommensurate. Then for all $f \in C(\Omega)$ and $\omega \in \Omega$,

$$\lim_{r\to\infty} \frac{1}{|B_r|} \int_{B_r} f(T_{-\mathbf{a}}\omega)\mathrm{d}\mathbf{a} = \int_\Omega f \mathrm{d}\mathbb{P} \qquad \text{(Birkhoff property)}$$

where B_r is the ball of radius r centered at zero.

Observables in a tight binding electron model: bilayer case

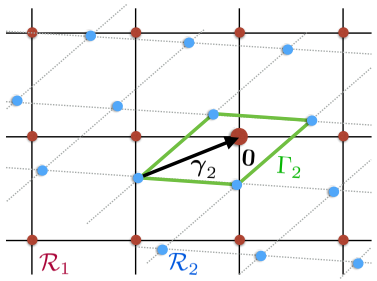

Minimal parameterization of operators by functions on the groupoid $\Gamma(X)$:

$$f_{11}: \quad \vec{\Gamma}_{11} = \Gamma_2 \times \mathcal{R}_1 \to \mathbb{C}, \qquad f_{12}: \quad \vec{\Gamma}_{12} \equiv \mathbf{R}^2 \to \mathbb{C},$$
$$f_{21}: \quad \vec{\Gamma}_{21} \equiv \mathbf{R}^2 \to \mathbb{C}, \qquad f_{22}: \quad \vec{\Gamma}_{22} = \Gamma_1 \times \mathcal{R}_2 \to \mathbb{C}.$$

- C^* algebra formulation [Bellissard, Shulz-Baldes, Prodan,...]
- Operator representation π_ω, sum, product rules including magnetic fields.

Trace and Averages

Proposition (E. Cancès, P. Cazeaux, M. Luskin)

- A trace per unit volume $\mathcal{T}$ is uniquely defined by

$$\mathcal{T}(f) = \lim_{R\to\infty} \frac{1}{\#\left(B_R \cap \mathcal{L}^\omega\right)} \mathrm{Tr}\left(\pi_\omega(f)|_{B_R}\right),$$

  where B_R is the ball of radius R centered at $\mathbf{0}$.
- This trace is also computed by the formula:

$$\mathcal{T}(f) = \frac{1}{|\Gamma_1| + |\Gamma_2|}\left(\int_{\Gamma_2} f_{11}(\gamma_2, \mathbf{0}) d\gamma_2 + \int_{\Gamma_1} f_{22}(\gamma_1, \mathbf{0}) d\gamma_1\right).$$

Also available: explicit, implementable formulae for

- differentiation: $(\partial_j f)(\omega, \mathbf{x}) = i x_j f(\omega, \mathbf{x})$,
- functional calculus: $\Phi(f) = \frac{1}{2\pi i} \oint_{\mathcal{C}} \Phi(z)(z - f)^{-1} dz$.

Electronic transport: a phenomenological model

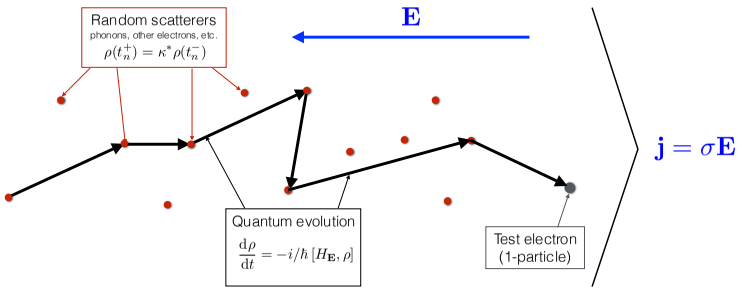

- Effective quantum Boltzmann equation [H. Schulz-Baldes & J. Bellissard, '94]:

$$\frac{\mathrm{d}\rho}{\mathrm{d}t} + \mathcal{L}_{h_{\mathbf{E}}}(\rho) = -\frac{1-\kappa^*}{\tau}(\rho), \quad \mathcal{L}_h(\cdot) = i/\hbar[h, \cdot].$$

- **Noncommutative Kubo formula** (Relaxation Time Approximation):

$$\sigma_{kl} = \left(\frac{e}{\hbar}\right)^2 \mathcal{T}\left(\partial_k h * (1/\tau_{rel} + \mathcal{L}_h)^{-1} \partial_l f_{\beta,\mu}(h)]\right).$$

A one-dimensional bilayer toy model

- Idea: two atomic chains with different lattice constants.

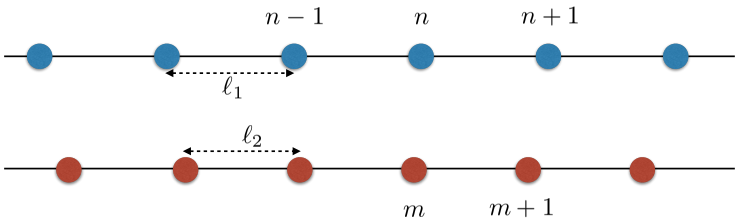

- Geometric normalization:

$$\ell_1 \ell_2 = 1.$$

Model Hamiltonian:

- Intra-chain interactions: nearest neighbor hopping with parameter 1,
- Distance-dependent inter-chains interactions:

$$t_{mn} = We^{-\frac{1}{2}\left(\frac{x_m - x_n}{\sigma}\right)^2}.$$

A one-dimensional bilayer toy model

- Idea: two atomic chains with different lattice constants.

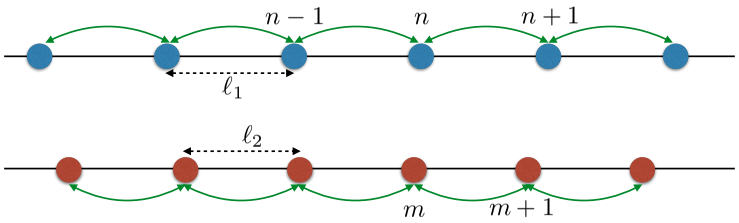

- Geometric normalization:

$$\ell_1 \ell_2 = 1.$$

Model Hamiltonian:

- Intra-chain interactions: nearest neighbor hopping with parameter 1,
- Distance-dependent inter-chains interactions:

$$t_{mn} = We^{-\frac{1}{2}\left(\frac{x_m - x_n}{\sigma}\right)^2}.$$

A one-dimensional bilayer toy model

- Idea: two atomic chains with different lattice constants.

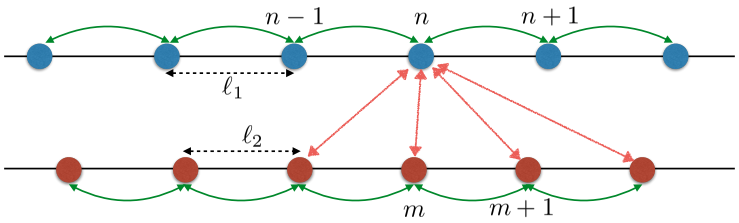

- Geometric normalization:

$$\ell_1 \ell_2 = 1.$$

Model Hamiltonian:

- Intra-chain interactions: nearest neighbor hopping with parameter 1,
- Distance-dependent inter-chains interactions:

$$t_{mn} = We^{-\frac{1}{2}\left(\frac{x_m - x_n}{\sigma}\right)^2}.$$

Density of States

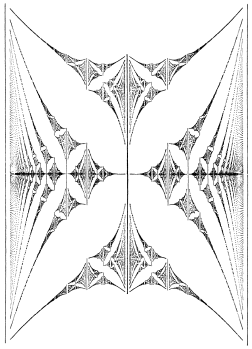

Hofstadter Butterfly
2D square lattice

[*Energy levels and wave functions of Bloch electrons in rational and irrational magnetic fields*, D. Hofstadter '76]

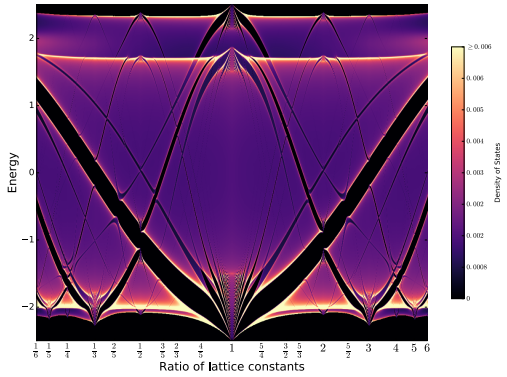

Density of states
1D IC model

Parameters: $\sigma = .25$ and $W = .5$.
Technique: Periodic approximants, Chebyshev polynomial expansion.

Calculation of the conductivity

Challenge: the noncommutative Kubo formula is expensive to compute:

$$\sigma_{kl} = \left(\frac{e}{\hbar}\right)^2 \mathcal{T}\left(\partial_k h * (1/\tau_{rel} + \mathcal{L}_h)^{-1} \partial_l f_{\beta,\mu}(h)]\right), \quad \mathcal{L}_h(\cdot) = i/\hbar[h, \cdot].$$

- Many parameters: τ_{rel}, β, μ.
- How to avoid repeating the full calculation for each parameter value?

Two-step approach:

- First, compute an intermediate quantity with no parameters: the current-current correlation measure,

$$\int_{\mathbf{R}^2} f(E)g(E')\mathrm{d}m_{kl}(E, E') = \mathcal{T}\left(f(h) \cdot \partial_k h \cdot g(h) \cdot \partial_l h\right).$$

- Then the conductivity is given as an integral with respect to $\mathrm{d}m_{kl}$:

$$\sigma_{kl} = \left(\frac{e}{\hbar}\right)^2 \int_{\mathbf{R}^2} \frac{f_{\beta,\mu}(E') - f_{\beta,\mu}(E)}{E - E'} \frac{\mathrm{d}m_{kl}(E, E')}{1/\tau_{rel} - i/\hbar(E - E')}.$$

Two-dimensional Chebyshev expansion

Exploration of the parameter space $\alpha = \ell_2/\ell_1$:

- Periodic structures with q atoms in chain 1, p in chain 2: $\alpha = p/q$,
- Assemble and diagonalize the Hamiltonian matrix for all $p + q = N$.

Step 1: computation of the Chebyshev moments of the measure m_{kl}:

$$\mathcal{M}^{\alpha}_{mn} = \frac{1}{N}\mathrm{Tr}\left(T_m(H_\alpha)\cdot\widetilde{\partial H_\alpha}\cdot T_n(H_\alpha)\cdot\widetilde{\partial H_\alpha}\right), \quad 0 \leqslant m, n \leqslant M.$$

- T_m are the Chebyshev polynomials: $T_0 = 1$, $T_1 = X$, $T_{m+1} = 2XT_m - T_{m-1}$.
- Efficient calculation thanks to the recurrence relation.

Step 2: Gauss-Chebyshev quadrature of the conductivity integral:

$$\sigma \approx \frac{1}{M^2}\sum_{k,l=0}^{M-1}\Gamma^{\alpha}_{kl}\Phi_{\beta,\mu,\tau_{\mathrm{rel}}}(ax_k + b, ax_l + b).$$

- $\Phi_{\beta,\mu,\tau_{\mathrm{rel}}}$ is the integrand in the spectral formula,
- Γ^{α}_{kl} are the raw cosine transform of the $\mathcal{M}^{\alpha}_{mn}$.

Conductivity

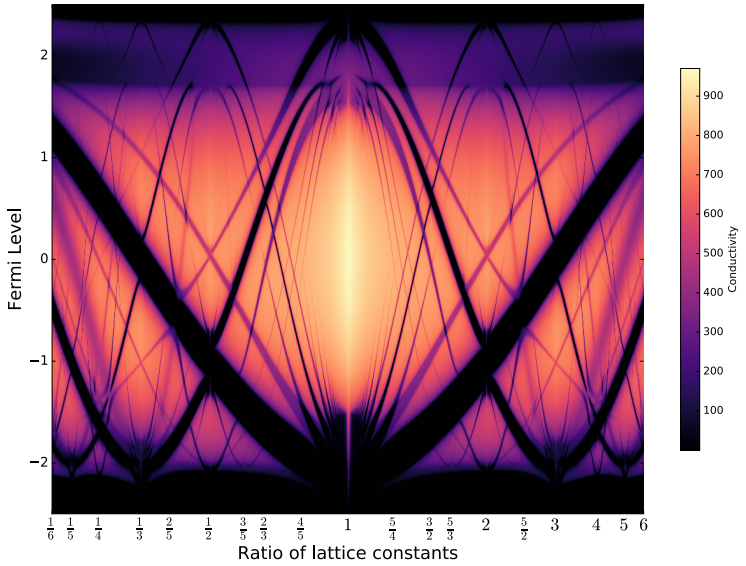

Conductivity

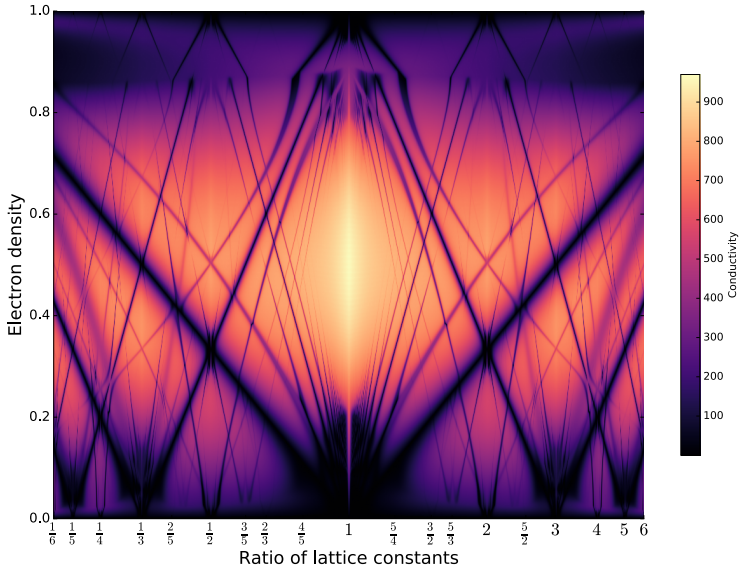

Other known formulae

- Frequency-dependent conductivity (Belissard et. al., JPM '94):

$$\sigma_{kl} = \left(\frac{e}{\hbar}\right)^2 \mathcal{T}\left(\partial_k h * (1/\tau_{rel} + i\omega + \mathcal{L}_h)^{-1} \partial_l \Phi_{FD}(h)\right)$$

- Chern number (Belissard et. al., JPM '94):

$$C = 2\pi i \mathcal{T}\left(P_F[\partial_1 P_F, \partial_2 P_F]\right). \tag{1}$$

- Spin-Chern number (Prodan, PRB'09):

$$C_s = \frac{1}{2}(C_+ - C_-), \quad C_\pm = 2\pi i \mathcal{T}\left(P_\pm[\partial_1 P_\pm, \partial_2 P_\pm]\right). \tag{2}$$

- Electric polarization (Schulz-Baldes and Teufel, arxiv '12)

$$\Delta P = \int_0^T dt \mathcal{T}\left(P_F(t)[\partial_t P_F(t), \nabla p(t)]\right) \tag{3}$$

- etc.

Surface Plasmon Polaritons in 2D materials: Engineering light at the nanoscale

- Plasmons beat the diffraction limit:
  - **sub-wavelength optics.**
- Strong localization of EM fields:
  - **nonlinear optics.**

- **Control electromagnetic energy in subwavelength scales:**
  - nano-waveguides, nano-antennas,
  - extremely small and ultrafast optic and electronic devices.
- High sensitivity to dielectric properties: sensors, detectors.

SPPs in 2D layers

- Classical description: **Time-harmonic Maxwell's equations**

$$\begin{cases} i\omega\varepsilon_0\mathbf{E} + \nabla \times (\mu_0^{-1}\mathbf{B}) = \mathbf{J}_a, & i\omega\nabla\cdot(\varepsilon_0\mathbf{E}) = \nabla\cdot\mathbf{J}_a, \\ -i\omega\mathbf{B} + \nabla\times\mathbf{E} = \mathbf{0}, & \nabla\cdot\mathbf{B} = \mathbf{0}. \end{cases}$$

- Jump condition on the interface Σ with effective surface conductivity $\sigma^{\Sigma}(\omega)$:

$$\begin{cases} \mathbf{n}\times\{\mathbf{E}^+ - \mathbf{E}^-\}\big|_\Sigma = \mathbf{0}, \\ \mathbf{n}\times\{(\mu_0^{-1}\mathbf{B})^+ - (\mu_0^{-1}\mathbf{B})^-\}\big|_\Sigma = \sigma^{\Sigma}(\omega)\{(\mathbf{n}\times\mathbf{E})\times\mathbf{n}\}\big|_\Sigma. \end{cases}$$

- **Resonant condition:** $\mathrm{Im}\ \sigma^{\Sigma}(\omega) \gg \mathrm{Re}\ \sigma^{\Sigma}(\omega)$.

SPPs in 2D layers

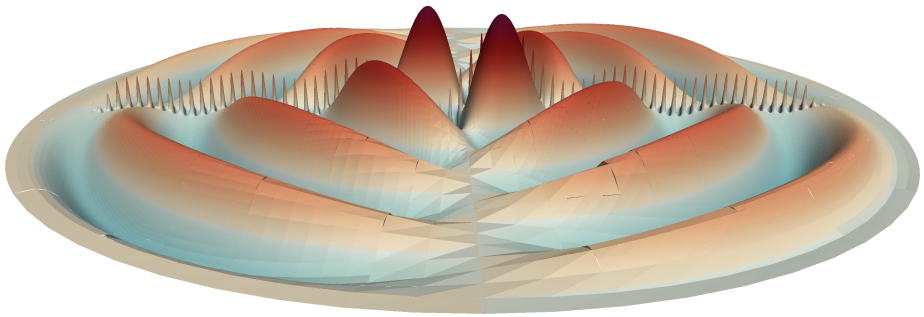

Representation of the electric field E_x in a plane cut perpendicular to the layer.
A dipole source excites a plasmon on a 2D metallic interface.

Numerical simulation by M. Maier, University of Minnesota.

- SPP modes have **very short wavelengths.**
- **Crucial ingredient: conductivity / dielectric response of the layer.**

Relaxation and small-angle Moire patterns

Goal: model, simulate and analyze relaxation patterns.

- Mesoscale Moire patterns at small angles.
- Specific diffraction patterns.

Challenges:

- Integrate into geometric framework?
- Efficient numerical simulations,
- Inverse problem (diffraction or real space images).

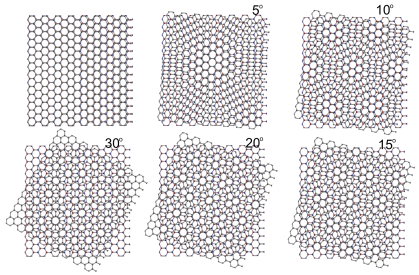

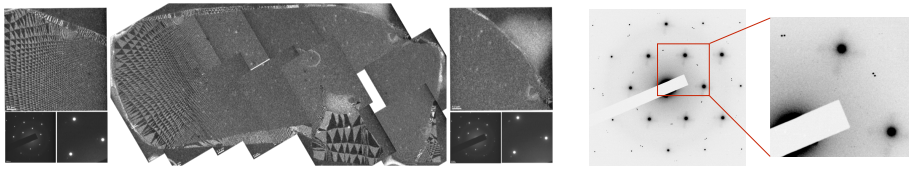

Twisted graphene bilayer encapsulated in hBN

[TEM Dark Field images: H. Yoo, P. Kim, Harvard University]

First steps: commensurate-incommensurate transition in 1D

- Analysis of 1D toy model
- Elastic relaxation of incommensurate chains
- Existence of ground states
- Numerical analysis

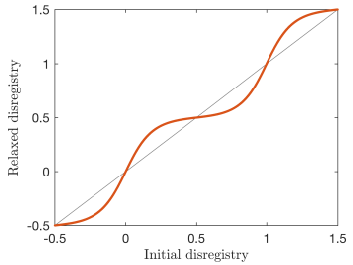

Parameters:

- $\alpha = \frac{8}{13}\frac{1+\sqrt{5}}{2}$
- Periodic approximant:

$|\alpha - p/q| < 10^{-7}$

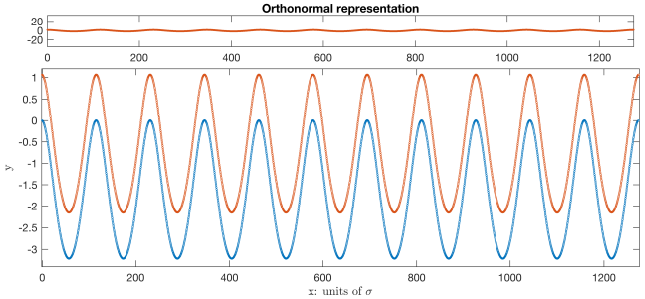

[P.Cazeaux, M. Luskin and E. Tadmor, Analysis of rippling in incommensurate 1D coupled chains, '16]

Summary

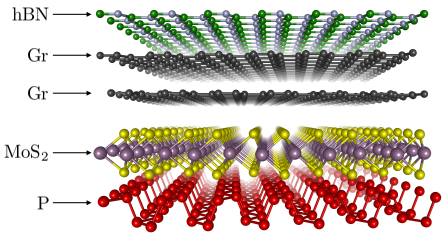

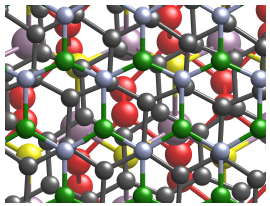

Top view of the atomic structure

- Current methods approximate incommensurate structures by supercells:
  - Size increases quickly for low angle twist, very expensive calculations
  - Uncontrolled and unknown error
- New methods sample configurations, exploit locality
  - Can efficiently compute full parameter space, even low angle twist
  - Efficient theory-based numerical methods with controlled and known error

Conclusion and perspectives

- Hull: minimal parameterization of configurations of incommensurate multilayer systems.
- Observables: C^*-algebras, abstract tool appropriate for incommensurate 2D heterostructures.

Future challenges:

- A lot of work to do to implement correctly the existing formulas, e.g.
  - Contour integrals,
  - Chebyshev polynomials,
  - Lanczos recursion chains,
  - Many other possibilities.

References

Georgios A. Tritsaris, Sharmila N. Shirodkar, Efthimios Kaxiras, Paul Cazeaux, Mitchell Luskin, Petr Plecháč, and Eric Cancès. Perturbation theory for weakly coupled two-dimensional layers. *Journal of Materials Research*, 31:959–966, 4 2016.

Daniel Massatt, Mitchell Luskin, and Christoph Ortner. Electronic density of states for incommensurate layers. *SIAM J. Multi. Model. & Sim.*, 15:476–499, 2017.

Stephen Carr, Daniel Massatt, Shiang Fang, Paul Cazeaux, Mitchell Luskin, and Efthimios Kaxiras. Twistronics: manipulating the electronic properties of two-dimensional layered structures through the twist angle. *Phys. Rev. B*, 95:075420, 2017.

Eric Cancès, Paul Cazeaux, and Mitchell Luskin. Generalized Kubo formulas for the transport properties of incommensurate 2D atomic heterostructures. *Journal of Mathematical Physics*, to appear.

Paul Cazeaux, Mitchell Luskin, and Ellad Tadmor. Analysis of rippling in incommensurate one-dimensional coupled chains. *SIAM J. Multi. Model. & Sim.*, 15:56–73, 2017.

Dio Margetis and Mitchell Luskin. On solutions of Maxwell's equations with dipole sources over a thin conducting film. *Journal of Mathematical Physics*, 57(4), 2016.

Matthias Maier, D. Margetis, and M. Luskin. Dipole excitation of surface plasmon on a conducting sheet: finite element approximation and validation. *J. Comput. Phys.*, 126–145, 2017.